

Sketching as a Tool for Understanding and Accelerating Self-attention for Long Sequences

Yifan Chen^{1*}, Qi Zeng^{1*}, Dilek Hakkani-Tur², Di Jin², Heng Ji¹, Yun Yang¹

¹University of Illinois Urbana-Champaign ²Amazon Alexa AI
¹{yifanc10, qizeng2, hengji, yy84}@illinois.edu
²{hakkanit, djinamzn}@amazon.com

Abstract

Transformer-based models are not efficient in processing long sequences due to the quadratic space and time complexity of the self-attention modules. To address this limitation, Linformer and Informer are proposed to reduce the quadratic complexity to linear (modulo logarithmic factors) via low-dimensional projection and row selection respectively. These two models are intrinsically connected, and to understand their connection, we introduce a theoretical framework of matrix sketching. Based on the theoretical analysis, we propose Skeinformer to accelerate self-attention and further improve the accuracy of matrix approximation to self-attention with three carefully designed components: column sampling, adaptive row normalization and pilot sampling reutilization. Experiments on the Long Range Arena (LRA) benchmark demonstrate that our methods outperform alternatives with a consistently smaller time/space footprint.¹

1 Introduction

Transformer (Vaswani et al. 2017) utilizes softmax self-attention modules to capture the dependency between tokens in a sequence and has been widely used in various Natural Language Processing tasks. The time and space complexity of the dot-product self-attention is quadratic in the input sequence length, which restricts the largest sequence length and batch size. To adapt transformers to long sequences, documents have to be truncated, chunked using a sliding window, or processed in parallel on multiple GPUs. These additional operations usually cause the loss of long-range dependency and introduce additional computational costs.

In this paper, we focus on efficient self-attention methods (Xiong et al. 2021; Qiu et al. 2020; Zaheer et al. 2020; Beltagy, Peters, and Cohan 2020; Kitaev, Kaiser, and Levskaya 2020; Roy et al. 2021), among which Linformer (Wang et al. 2020a) and Informer (Zhou et al. 2020) are two representative approaches to reducing the $\mathcal{O}(n^2)$ self-attention to an $\tilde{\mathcal{O}}(n)$ operation ($\tilde{\mathcal{O}}(\cdot)$ means $\mathcal{O}(\cdot)$ modulo poly-log terms and n is the sequence length) in both space and time complexity. Linformer forms a low-rank factorization of the original attention by decomposing it into

smaller attentions, while Informer allows each key to only attend to a certain number of queries.

To better understand self-attention, we introduce a theoretical framework, sketching (Woodruff et al. 2014), to help explain the key ideas in Informer and Linformer from the perspective of matrix approximation. Specifically, sketching methods replace the original matrix B with its random sketch BS to reduce computations. In Section 3.3 we introduce some concrete instances of commonly used distributions for constructing the random sketching matrix S . Furthermore, taking matrix approximation as a general guideline, we recognize the deficiency in Informer and Linformer, that they either do not fully utilize the information in the value matrix V , or deviate from the original self-attention output. This guideline also motivates us to propose **Skeinformer** through the theoretical analysis under the sketching framework.

To improve the approximation accuracy in terms of the original attention output, Skeinformer applies sub-sampling sketching to reduce time complexity and exploits the information from the value matrix V with **column sampling**. Skeinformer also incorporates an **adaptive row normalization** step, which approximates the un-selected rows by a vector with all elements $\frac{1}{n}$ and has significantly boosted the performance of Informer. In addition, we introduce a simple yet effective step, **pilot sampling reutilization**, which reuses the computation of pilot sampling to improve both the approximation accuracy and training efficiency. Our experiments on the LRA benchmark show that Skeinformer consistently uses less space and time while achieving better accuracy than most baseline methods.

In summary, our contributions are twofold:

- We introduce sketching as a theoretical framework for analyzing and developing efficient transformers. Specifically, the randomized sketching theory covers these two methods from the perspective of approximate matrix multiplication. This framework connects the studies on efficient transformers and randomized sketching theory, so that future development in efficient transformers and sketching can benefit each other.
- We propose Skeinformer as a straightforward product of the sketching framework to accelerate the training and inference of transformers. Skeinformer consists of three components: the initial column sampling that incorpo-

*Equal contribution.

¹Our code is released at

<https://github.com/pkuzengqi/Skeinformer>

rates the information from the value matrix V into the sampling probabilities, the adaptive row normalization that fills un-selected columns with the averaged selected columns, and the pilot sampling re-utilization.

2 Related work

The ability to process long sequences is critical for many Natural Language Processing tasks, including Document Summarization (Xiao and Carenini 2019; Huang et al. 2021), Question Answering (Wang et al. 2020b), Information Extraction (Li, Ji, and Han 2021; Du and Cardie 2020; Ebner et al. 2020), and Machine Translation (Bao et al. 2021). However, the quadratic computational cost of self-attention in transformer-based models limits their application in long-sequence tasks. Recent methods have been proposed to accelerate attention computation by selectively attending to a subset of the tokens or with low-rank matrix approximation. We refer readers to a survey paper on efficient transformers (Tay et al. 2020b) for more details on attention approximation methods.

Selective attention methods limit the scope of matrix operation with sparse attention patterns or column/row sampling methods. BlockBERT (Qiu et al. 2020) introduces sparse block structures into the attention matrix. Sparse Transformer (Child et al. 2019) introduces dilated patterns. Big Bird (Zaheer et al. 2020) proposes a combination of random, window, and global attention. Longformer (Beltagy, Peters, and Cohan 2020) combines local windowed attention with task-motivated global attention. The most related work to ours is Informer (Zhou et al. 2020), which allows each key to only attend to the top queries under the Kullback-Leibler divergence based sparsity measurement.

Low-rank attention matrix approximation methods are based on the assumption of low-rank structure in the full self-attention matrix. Linformer (Wang et al. 2020a) compresses the size of the key and value matrices by the Johnson-Lindenstrauss transform (Johnson and Lindenstrauss 1984). Performer (Choromanski et al. 2020) recognizes the attention score matrix as an empirical Gaussian kernel matrix and constructs a low-rank projection for both the query and key matrices through random Fourier features (Rahimi, Recht et al. 2007). Nyströmformer (Xiong et al. 2021) instead utilizes Nyström method (Williams and Seeger 2001; Drineas, Mahoney, and Cristianini 2005) to approximate the attention score matrix.

Some other methods follow a similar principle to decompose the attention score matrix, although they are not necessarily aiming to approximate the original self-attention itself. The representative methods include Linear Transformer (Katharopoulos et al. 2020), which claims that the exponential transform of the dot-product in the softmax operation can be replaced by the direct matrix multiplication of the projected query and key matrices, and Reformer (Kitaev, Kaiser, and Levskaya 2019), which forces the query and key matrices to be identical and applies locality-sensitive hashing (LSH) (Har-Peled, Indyk, and Motwani 2012) to simplify the computation of the attention score matrix. Those methods are effective alternatives of the original self-attention, while they do not fall into the scope of matrix ap-

proximation. We spare the discussion of those methods in this paper.

3 Sketching Framework for Self-Attention

3.1 Problem formulation

Given an input sequence $X \in \mathbb{R}^{n \times d_{input}}$, where n is the sequence length and d_{input} is the embedding dimension, the dot-product attention for a single attention head in transformer (Vaswani et al. 2017) is defined as

$$\text{Attention}(Q, K, V) = \text{softmax}\left(\frac{QK^T}{\sqrt{p}}\right)V = D^{-1}AV$$

where $Q = XW_Q$, $K = XW_K$, and $V = XW_V$. W_Q , W_K , $W_V \in \mathbb{R}^{d_{input} \times p}$ are the query, key, and value weight metrics that linearly project the input X of dimension d_{input} to an output tensor of dimension p .

To ease the future analysis, the softmax term can be rewritten into $D^{-1}A$, where $A := \exp(QK^T/\sqrt{p})$, and D is a diagonal matrix whose diagonal is $\exp(QK^T/\sqrt{p}) \cdot \mathbf{1}$ ($\mathbf{1}$ is a size- n vector with all elements being 1).

3.2 Sketching methods

Beyond current attempts to accelerate self-attention, research in the random matrix approximation community can be potentially applied to fast attention. Among the theoretical frameworks, the sketching method (Woodruff et al. 2014) is the most comprehensive one as its general concept can incorporate many different approaches.

The core idea of the sketching method is to replace an original matrix $B \in \mathbb{R}^{n_B \times n}$ with its random sketch BS , where $S \in \mathbb{R}^{n \times d}$ is a random sketching matrix. In practice, to apply the sketching method we plug an identity matrix into the original expression, and then formally replace the identity matrix with the product SS^T , as the distribution of S is usually designed to satisfy the constraint that

$$\mathbb{E}(SS^T) = I. \quad (1)$$

Common methods to construct a sketching matrix include sub-Gaussian maps (Vershynin 2010; Halko, Martinsson, and Tropp 2011), subsampled randomized Hadamard transform (SRHT) (Ailon and Chazelle 2006; Lu et al. 2013; Yang et al. 2017), sparse oblivious subspace embeddings (Cohen, Nelson, and Woodruff 2016), very sparse random projection (Li, Hastie, and Church 2006), accumulative sketching (Chen and Yang 2021), and sub-sampling sketching (Monte Carlo algorithms) (Drineas, Kannan, and Mahoney 2006). Specifically, Informer and Linformer, two efficient transformer-based methods mentioned above, can be understood as applications of sub-sampling sketching and sub-Gaussian maps, respectively. We further elaborate the connections in the next subsection.

3.3 Sketching in self-attention approximation

A naïve step in applying sketching method to approximate the self-attention output $D^{-1}AV$ is to construct a random sketch of the un-normalized attention score matrix A , the bottleneck in computation. Informer and Linformer construct two types of sketches, $A^T S$ and AS respectively.

Algorithm 1: Skeinformers.

- Input:** query matrix \mathbf{Q} , key matrix \mathbf{K} , value matrix \mathbf{V} (all are n -by- p), and sub-sample size d
Output: Attention output matrix \mathbf{R} with the same shape as \mathbf{V}
- 1 Uniformly sample d indices j_1, \dots, j_d with replacement;
 - 2 Construct the $d \times p$ matrix \mathbf{Q}_J as to the index set $J := \{j_k\}_{k=1}^d$, whose k -th row is $\mathbf{Q}_{(j_k)}$;
 - 3 Compute the matrix $\mathbf{B}_J = \text{softmax}(\mathbf{Q}_J \mathbf{K}^T / \sqrt{p})$; // pilot sampling
 - 4 Based on \mathbf{B}_J , give the estimated sub-sampling probabilities $\{\hat{p}_i\}_{i=1}^n$ as in Equation (5);
 - 5 With $\{\hat{p}_i\}_{i=1}^n$ sample d indices j'_1, \dots, j'_d without replacement;
 - 6 Construct the d -by- p matrix $\mathbf{K}_{J'}$ (resp., $\mathbf{V}_{J'}$) according to the indices list $J' := \{j'_k\}_{k=1}^d$, whose k -th row is $\mathbf{K}_{(j'_k)}$ (resp., $\mathbf{V}_{(j'_k)}$);
 - 7 Compute the two matrices $\mathbf{A}^{J'} = \exp(\mathbf{Q} \mathbf{K}_{J'}^T / \sqrt{p})$, and $\mathbf{R}_{J'} = \mathbf{A}^{J'} \mathbf{V}_{J'}$; // column sampling
 - 8 Construct a length n column vector \mathbf{g} whose i -th element is $(\prod_{k=1}^d a_{ij'_k})^{\frac{1}{d}}, \forall i \in [n]$;
 - 9 Compute the row sum vector $\mathbf{d} := \mathbf{A}^{J'} \mathbf{1}_d + (n-d)\mathbf{g}$; // adaptive row normalization
 - 10 Denote the un-selected part of \mathbf{V} as $\mathbf{V}_{(J')^c}$, and compute the vector $\mathbf{v} = \mathbf{V}_{(J')^c}^T \mathbf{1}_{n-d}$;
 - 11 Obtain the intermediate output $\mathbf{R} = \text{diag}(\mathbf{d}^{-1})(\mathbf{R}_{J'} + \mathbf{g}\mathbf{v}^T)$, where \mathbf{d}^{-1} is the element-wise inverse of \mathbf{d} ;
 - 12 Compute $\mathbf{B}_J \mathbf{V}$ and assign it to the corresponding rows of \mathbf{R} ; // pilot sampling reutilization
 - 13 Return the matrix \mathbf{R} as the ultimate output of this algorithm;
-

Informer Informer selects d important rows of $\mathbf{D}^{-1} \mathbf{A}$, though deterministically, to represent $\mathbf{D}^{-1} \mathbf{A}$. This process can be related to a sketched approximation $\mathbf{D}^{-1} \mathbf{S} \mathbf{S}^T \mathbf{A}$, where \mathbf{S} is a sub-sampling matrix defined as follows:

Definition 3.1 (Sub-sampling matrix). *Consider a discrete distribution which draws i with probability $p_i > 0, \forall i \in [n]$. For a random matrix $\mathbf{S} \in \mathbb{R}^{n \times d}$, if \mathbf{S} has independent and identically distributed (i.i.d.) columns and each column $\mathbf{S}^{(j)}$ is $\frac{1}{\sqrt{d p_i}} \mathbf{e}_i$ with probability p_i , where \mathbf{e}_i is the i -th column of the n -by- n identity matrix \mathbf{I}_n , then \mathbf{S} is called a sub-sampling matrix with sub-sampling probabilities $\{p_i\}_{i=1}^n$.*

Some researchers in the field of approximate matrix multiplication have provided a practical guideline for the choice of the sub-sampling probabilities $\{p_i\}_{i=1}^n$ in \mathbf{S} . Specifically for the matrix multiplication \mathbf{BC} of two arbitrary matrices \mathbf{B} and \mathbf{C} , Drineas, Kannan, and Mahoney (2006) approximate it with $\mathbf{B} \mathbf{S} \mathbf{S}^T \mathbf{C}$ and set the sampling probability p_i in \mathbf{S} proportional to the product $\|\mathbf{B}^{(i)}\|_2 \|\mathbf{C}_{(i)}\|_2$, where $\mathbf{B}^{(i)}$ is the i -th column in matrix \mathbf{B} and $\mathbf{C}_{(i)}$ is the i -th row in matrix \mathbf{C} . For the product $\mathbf{D}^{-1} \mathbf{A}$, the probability in sketching will be $p_i = \frac{\sqrt{\sum_{j=1}^n a_{ij}^2}}{\sum_{j=1}^n a_{ij}}$, where a_{ij} is the j -th element of the i -th row in matrix \mathbf{A} .

The above sampling probability choice $\{p_i\}_{i=1}^n$ is highly related to the sparsity measurement used in Informer, which is $M_i = \ln \frac{\sum_{j=1}^n a_{ij}}{(\prod_{j=1}^n a_{ij})^{1/n}}$. Here p_i is the ratio between the quadratic mean and the arithmetic mean of $\{a_{ij}\}_{j=1}^n$; M_i is the logarithm of the ratio between the arithmetic mean and the geometric mean. It is clear that M_i will increase with p_i as these two ratios will both be large when $\{a_{ij}\}_{j=1}^n$ are highly non-uniform. We conclude that in Informer, the main idea to select the rows with high sparsity measurement can be taken as a special variant of the sub-sampling method above with probabilities $\{p_i\}$.

Linformer Another type of sketch \mathbf{AS} is mentioned (but not finally used) in Linformer. The sketching matrix \mathbf{S} takes a form different from sub-sampling. The construction of \mathbf{S}

in Linformer is motivated by Johnson-Lindenstrauss (JL) transform, which applies the sketching matrix \mathbf{S} satisfying the (ε, δ) -JL guarantee:

Definition 3.2 (Oblivious Johnson-Lindenstrauss guarantee (Johnson and Lindenstrauss 1984)). *A distribution \mathcal{D} over $\mathbb{R}^{n \times d}$ satisfies “oblivious Johnson-Lindenstrauss guarantee” if for some $\varepsilon, \delta \in (0, 1/2)$:*

$$\forall \mathbf{b} \in \mathbb{R}^n, \mathbb{P}_{\mathbf{S} \sim \mathcal{D}} (\|\mathbf{S} \mathbf{b}\|_2^2 - \|\mathbf{b}\|_2^2| > \varepsilon \|\mathbf{b}\|_2^2) < \delta. \quad (2)$$

Specifically, a matrix with i.i.d. Gaussian elements can meet the above requirement. It has been proven (Johnson and Lindenstrauss 1984) that with $d = \mathcal{O}(\varepsilon^{-2} \log(1/\delta))$, a Gaussian sketching matrix \mathbf{S} can satisfy the oblivious (ε, δ) -JL guarantee. To extend the conclusion from a single vector $\mathbf{b} \in \mathbb{R}^n$ to a matrix $\mathbf{B} \in \mathbb{R}^{n_B \times n}$, the size d still needs to suffer from an additional $\log n_B$ term (Vershynin 2010), which matches the bound in sub-sampling sketching (Drineas, Kannan, and Mahoney 2006, Theorem 1).

However, the direct use of Gaussian sketching matrix, i.e. the approximation $\mathbf{D}^{-1} \mathbf{A} \mathbf{S} \mathbf{S}^T \mathbf{V}$ (Wang et al. 2020a, Eqn. (5)), requires the computation of the whole matrix \mathbf{A} . To avoid this computational burden, Linformer replaces the form of sketching method with $\text{softmax}((\mathbf{Q} \mathbf{K}^T / \sqrt{p}) \mathbf{S}) \mathbf{S}^T \mathbf{V}$, which sacrifices the accuracy for efficiency in some tasks as shown in later experimental results.

4 Methodology: Skeinformers

Based on the previous discussion, we observe that Informer omits the information from the value matrix \mathbf{V} , and Linformer deviates from the usual sketching form for efficiency. To address these issues and fully exploit the power of sketching, we strengthen the attention approximation with the following components.

In Section 4.1, we introduce column importance sampling, which allows the information incorporation from \mathbf{V} and accelerate the matrix multiplication (compared to JL transform); in Section 4.2 and Section 4.3, we leverage

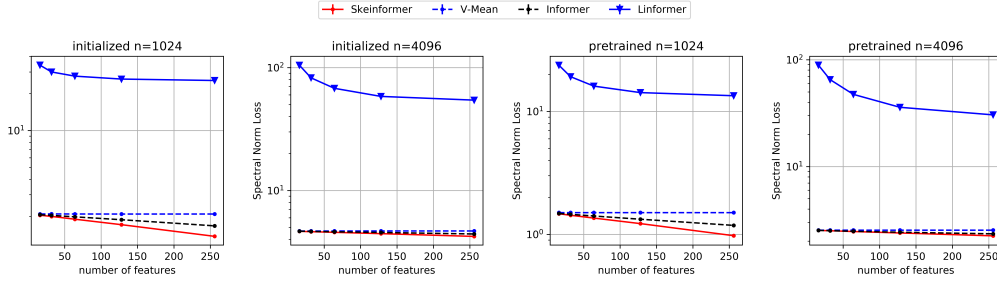


Figure 1: Spectral norm results with the sequence length of 1024 and 4096. Y axis: Lower percentage score means better approximation. X axis: Higher number of feature means larger computation cost.

the sampled columns to perform the row normalization and reuse the pilot row sampling, which further improves the approximation and makes the training more stable.

We describe the proposed method **Skeinformer** in Algorithm 1 and verify its performance on matrix approximation in Section 5. We also provide complexity analysis in Section 4.5 to show that our method enjoys the same $\mathcal{O}(n \log n)$ complexity as other methods.

4.1 Column sampling

The row selection in Informer has been derived as a special variant of the sketching method and can be further improved by utilizing the information from \mathbf{V} , in a form similar to Linformer:

$$\mathbf{D}^{-1} \mathbf{A} \mathbf{S} \mathbf{S}^T \mathbf{V},$$

where \mathbf{S} above is a sub-sampling matrix defined in Definition 3.1 with sampling probabilities

$$p_i \propto \|(\mathbf{D}^{-1} \mathbf{A})^{(i)}\|_2 \|V_{(i)}\|_2, \quad i = 1, 2, \dots, n.$$

We remark that using the sub-sampling sketching in this way can both circumvent the computation burden of Gaussian sketching, and also allow the incorporation of the information from \mathbf{V} .

As \mathbf{S} formally samples some columns from $\mathbf{D}^{-1} \mathbf{A}$, we name the procedure as column sampling in our method. The performance regarding the Frobenius norm loss of the approximate matrix multiplication can be guaranteed by the following proposition:

Proposition 1 (Adapted from Theorem 1 (Drineas, Kannan, and Mahoney 2006)). *Suppose the attention score matrix $\mathbf{B} := \mathbf{D}^{-1} \mathbf{A} \in \mathbb{R}^{n \times n}$, the value matrix $\mathbf{V} \in \mathbb{R}^{n \times p}$, the number of sampled columns $d \in \mathbb{Z}^+$ such that $1 \leq d \leq n$, and the sampling probabilities $\{p_i\}_{i=1}^n$ are such that $\sum_{i=1}^n p_i = 1$ and such that for a quality coefficient $\beta \in (0, 1]$*

$$p_i \geq \beta \frac{\|B^{(i)}\| \|V_{(i)}\|}{\sum_{i'=1}^n \|B^{(i')}\| \|V_{(i')}\|}, \quad \forall i \in [n]. \quad (3)$$

Construct a sub-sampling matrix $\mathbf{S} \in \mathbb{R}^{n \times d}$ with sub-sampling probabilities $\{p_i\}_{i=1}^n$ as in Definition 3.1, and let $\mathbf{B} \mathbf{S} \mathbf{S}^T \mathbf{V}$ be an approximation to $\mathbf{B} \mathbf{V}$. Let $\delta \in (0, 1)$ and

$\eta = 1 + \sqrt{(8/\beta) \log(1/\delta)}$. Then with probability at least $1 - \delta$,

$$\|\mathbf{B} \mathbf{V} - \mathbf{B} \mathbf{S} \mathbf{S}^T \mathbf{V}\|_F^2 \leq \frac{\eta^2}{\beta d} \|\mathbf{B}\|_F^2 \|\mathbf{V}\|_F^2. \quad (4)$$

Remark. Proposition 1 guides Informer and our method to pick the important rows and columns of the attention score matrix \mathbf{B} . In self-attention, it is feasible to compute the norm $\|V_{(i')}\|$ of each row in \mathbf{V} with $\mathcal{O}(n)$ time, assuming the dimension p in each head is fixed and independent of n . However, similar to Informer, it is inefficient to exactly compute the ℓ_2 norm of each column in the n -by- n matrix \mathbf{B} , and we need pilot sampling as well to estimate the norm of the columns in \mathbf{B} . We show that $\mathcal{O}(\log n)$ samples in the pilot sampling is sufficient to guarantee the quality coefficient $\beta \geq \sqrt{\frac{1}{3}}$ with high probability by the following lemma. (The proof is deferred to Appendix B.)

Lemma 1. *Assume for any $i \in [n]$, $\|B^{(i)}\|^2/n$ is uniformly lower bounded by a constant C , where $\mathbf{B} := \mathbf{D}^{-1} \mathbf{A}$. For another constant $\delta \in (0, 1/2)$, we uniformly sample d indices $\{j_k\}_{k=1}^d$ from $[n]$ with replacement, and let d be a constant multiple of $\log(n/\delta)$. Then with probability at least $1 - \delta$, the estimated sub-sampling probabilities*

$$\hat{p}_i := \frac{(\sum_{k=1}^d b_{j_k i}^2)^{\frac{1}{2}} \|V_{(i)}\|}{\sum_{i'=1}^n (\sum_{k=1}^d b_{j_k i'}^2)^{\frac{1}{2}} \|V_{(i')}\|}, \quad \forall i \in [n], \quad (5)$$

satisfy the constraints (3) with $\beta = \sqrt{\frac{1}{3}}$, where b_{j_i} is the element of \mathbf{B} from the j -th row and i -th column.

This lemma states the sub-sampling weights used in our proposed method. Its computation only requires accesses to $\{B^{(j_k)}\}_{k=1}^d$ obtained from the pilot sampling, and thus has greatly reduced the time cost. Combining the preceding lemma and Proposition 1, we conclude that with the sampling probabilities $\{\hat{p}_i\}_{i=1}^n$ estimated by $\mathcal{O}(\log n)$ pilot samples, the sampled d important columns suffice to capture the essence of the original output $\mathbf{B} \mathbf{V}$. We close this subsection with a remark that the theoretical result that sub-sampling sketching can well approximate the original self-attention, indeed matches the rank collapse phenomenon observed by Dong, Cordonnier, and Loukas (2021) that self-attention can be well approximated by a low-rank matrix.

4.2 Adaptive row normalization

In addition to the theoretical guarantee of the sub-sampling sketching method, we identify an important component behind Informer, row normalization, which implicitly fills the un-selected rows with $\frac{1}{n}$. Toy experiments in Section 5 reveal that even the rank-one pure row normalization benchmark $\frac{1}{n}\mathbf{1}\mathbf{1}^T\mathbf{V}$, as an ablation, will have acceptable spectral norm loss $\|\mathbf{D}^{-1}\mathbf{A}\mathbf{V} - \frac{1}{n}\mathbf{1}\mathbf{1}^T\mathbf{V}\|_2$. Therefore, we incorporate adaptive row normalization to provide an even better attention score distribution in each row. It fills un-selected columns with the averaged selected columns. Moreover, from the model training perspective, it allows the whole value matrix \mathbf{V} in Skeinformers to participate in the computation (compared to only using the sub-sampling sketch $\mathbf{S}^T\mathbf{V}$), and thus can improve the efficiency of updating \mathbf{W}_V during the training.

Specifically, in adaptive row normalization any row in the matrix \mathbf{A} can be divided into two parts, the exactly computed elements in the selected columns with indices $\{j'_k\}_{k=1}^d \subset [n]$ and the other elements in the un-selected columns. For the latter, in each row, we set all the un-selected elements as the geometric mean of the selected ones, considering the exponentiation in softmax. We then perform row normalization based on the above construction, in which the i -th diagonal element in \mathbf{D} is estimated as

$$\hat{d}_{ii} = \sum_{k=1}^d a_{ij'_k} + (n-d) \left(\prod_{k=1}^d a_{ij'_k} \right)^{\frac{1}{d}}, \quad (6)$$

where each a_{ij} is the corresponding element in matrix \mathbf{A} . Next we normalize rows composed of exact elements in the selected columns, and the other elements estimated with the mean value above. We comment that though the component of adaptive row normalization makes the proposed method inapplicable to Proposition 1, it benefits the performance on matrix approximation and avoid the cost to compute the diagonal normalization matrix \mathbf{D} . (c.f. Section 5)

4.3 Pilot sampling reutilization

Since we have already computed \mathbf{B}_J in pilot sampling step (defined in Ln. 3 of Algorithm 1), we can exactly reproduce the d rows in the original self-attention output with an additional product $\mathbf{B}_J\mathbf{V}$ in $\mathcal{O}(n \log n)$ time. This allows for more precise approximation with little cost. In addition, the computation of those rows involves the whole key matrix \mathbf{K} , which benefits the training of the parameters \mathbf{W}_K .

4.4 Implementation Details

Applying the sub-sampling-based methods requires the support for padding masks commonly used in Natural Language Processing tasks. However, a naïve implementation of Algorithm 1 will result in the unnecessary sampling of the padding tokens. Therefore, we count the number of the unpadded tokens m , and only perform the pilot sampling within the certain range $[m]$. After the matrix \mathbf{B}_J is computed, we set its columns belonging to the padded part to be all zero, so that the probability \hat{p}_i of choosing column i from the padded part will be zero and the column will not be sampled in the later importance sampling. Similar modifications

can also be applied to Informer to enable its applications in NLP tasks in Section 6.

4.5 Complexity analysis

With the mild assumption in Lemma 1, we claim that our method can have an $\mathcal{O}(n \log n)$ time and space complexity. The claim is shown by the following analysis of the complexity, which heavily relies on the notations in Algorithm 1.

First, we point out that the row/column retrieving operation after index sampling can be implemented by only forming a view and thus the cost is negligible. For Line 1 ~ 4 in Algorithm 1, the time complexity of the uniform pilot sampling is $\mathcal{O}(d) = \mathcal{O}(\log n)$, while the computation of the matrix \mathbf{B}_J and the corresponding probabilities $\{\hat{p}_i\}_{i=1}^n$ costs $\mathcal{O}(nd) = \mathcal{O}(n \log n)$ time and space. For Lines 5 ~ 7, with probabilities $\{\hat{p}_i\}_{i=1}^n$, the importance sampling takes $\mathcal{O}(n + d \log n) = \mathcal{O}(n)$ time, and similar to the computation above it takes $\mathcal{O}(n \log n)$ time and space to obtain $\mathbf{A}_{J'}$ and $\mathbf{R}_{J'}$. For Lines 8 ~ 10, it is clear that the three vectors \mathbf{g} , \mathbf{d} , and \mathbf{v} can be computed in $\mathcal{O}(n \log n)$ time. As for the last step in Line 11, since it just requires the matrix product involving a diagonal matrix, we can finish the computation also in $\mathcal{O}(n \log n)$ time and space. In summary, the total time and space complexity for Algorithm 1 is at most $\mathcal{O}(n \log n)$, much lower than the $\mathcal{O}(n^2)$ complexity for the original softmax self-attention.

Remark. The complexity above is derived based on the high probability bound in Proposition 1, which is different than the derivation by some previous methods to claim the linear $\mathcal{O}(n)$ complexity.

5 Approximation Evaluation

As a preliminary justification of our proposed methods, we compute the spectral norm loss, a common metric for approximate matrix multiplication, to evaluate the effect of different models to approximate the original self-attention. We compare the spectral norms of the differences between the outputs from vanilla self-attention and other fast attention methods given the same input $\mathbf{Q}, \mathbf{K}, \mathbf{V}$. Specifically we compute $\|\mathbf{B}\mathbf{V} - \mathbf{R}\|_2$, where $\mathbf{B} := \mathbf{D}^{-1}\mathbf{A}$ is the attention score matrix in the original method, and \mathbf{R} is the output of each approximation method.

The inputs $\mathbf{Q}, \mathbf{K}, \mathbf{V}$ are constructed in the following process: We first truncate the raw text of sequence length 1024 or 4096 from Wikitext-2 dataset (Merity et al. 2017) into sequences of length 512 and embed the tokenized input with the embedding layer in a pretrained bert-base-cased model using Huggingface’s implementation (Wolf et al. 2019). Then we transform the input X into $\mathbf{Q}, \mathbf{K}, \mathbf{V}$ with the query, key, and value weight matrices from a pretrained model or a randomly initiated model.

We report the spectral norm loss of different sketching-based methods in Figure 1. The results are averaged over 768 trials, and the error bars in the figure represent the standard error of the reported values. For size d (x -axis) in the simulation, either the number of columns/rows selected or the projection dimension, it is set in the range from 2^3 to 2^8 .

A special baseline “V-Mean” always uses a rank-one matrix $\frac{1}{n}\mathbf{1}\mathbf{1}^T\mathbf{V}$ to approximate the original self-attention, and

Models	Text	ListOps	Retrieval	Pathfinder	Image	Average
Standard (Vaswani et al. 2017)	57.69	38.15	80.10	73.59	37.97	57.50
· w/o dropout	59.44	38.17	79.35	72.35	37.58	57.38
V-mean	65.29	28.78	80.49	61.01	34.33	53.98
BigBird (Zaheer et al. 2020)	61.91	38.86	79.73	71.75	35.00	57.45
Performer (Choromanski et al. 2020)	57.67	37.70	75.69	56.50	37.40	52.99
Nystromformer (Xiong et al. 2021)	60.91	37.76	79.87	72.53	31.93	56.60
Reformer (Kitaev, Kaiser, and Levskaya 2020)	62.69	37.94	78.85	69.21	36.42	57.02
Linformer (Wang et al. 2020a)	58.52	37.97	77.40	55.57	37.48	53.39
· w/ unreduced JLT	59.12	37.48	79.39	68.45	35.96	56.08
Informer (Zhou et al. 2020)	61.55	38.43	80.88	59.34	36.55	55.35
· w/ padding mask	60.98	37.26	79.92	62.51	37.19	55.57
Skeinformer	62.47	38.73	80.42	71.51	37.27	58.08
· w/ uniform sampling	64.48	30.02	80.57	64.35	36.97	55.28
· w/o row normalization	60.67	37.69	78.67	66.35	37.06	56.09
· w/ simple row normalization	60.26	38.35	78.97	65.41	39.72	56.54
· w/o pilot sampling reutilization	62.39	38.12	79.88	71.53	37.20	57.83

Table 1: Classification accuracy (%) on the test sets of LRA benchmark.

thus its approximation error does not change with the size d . “V-Mean” can also be seen as an ablation for the row normalization step (equivalent to adaptive row normalization without any sub-samples). From the results we observe the row normalization step greatly contributes to the approximation of self-attention that involving a softmax structure. Among the candidates, Skeinformer tends to have the smallest spectral norm loss, especially when d is large. We conclude that our algorithm design attains a higher accuracy than Informer and Linformer (shown in Figure 1), regarding the performance of matrix approximation.

6 Experiment

6.1 Setup

We compare our method with the standard quadratic self-attention (Vaswani et al. 2017), Big Bird (Zaheer et al. 2020), Linformer (Wang et al. 2020a), Informer (Zhou et al. 2020), Performer (Choromanski et al. 2020), and Nyströmformer (Xiong et al. 2021). In addition to their vanilla implementations, we compare with standard self-attention without dropout (since most fast attention methods do not have this component), Linformer with unreduced Johnson-Lindenstrauss Transform (the original form that Linformer deviates from), and Informer with padding masks (as introduced in 4.4). “V-Mean” always uses a rank-one matrix $\frac{1}{n}\mathbf{1}\mathbf{1}^T V$ to approximate the original self-attention, and serves as a special baseline against sampling.

To justify the effectiveness of the proposed components, we perform ablation studies, including replacing the column importance sampling with uniform sampling, disabling the adaptive row normalization or replacing it with the simple row normalization implemented in Informer, and disabling the pilot sampling reutilization.

Since some methods cannot be analyzed under the sketching framework, and their complexity is derived under different theoretical settings, we compare their practical performance through experiments on Long Range Arena (LRA) benchmark (Tay et al. 2020a). LRA is designed for long-context scenarios, and will be more appropriate for evalu-

ating efficient transformers for long sequences than more general Natural Language Understanding tasks with much shorter input context. We evaluate on five classification tasks in LRA benchmark: ListOps (Nangia and Bowman 2018), Text Classification on IMDb review dataset (Maas et al. 2011), Document Retrieval on AAN dataset (Radev et al. 2013), Pathfinder (Linsley et al. 2018), and Image Classification (Krizhevsky, Hinton et al. 2009)

6.2 Implementation details

As it is not realistic to exhaustively fine-tune all models and search for the best performance under limited computation resources, we instead replace the self-attention module in transformer with the various drop-in attention methods and keep other experimental settings the same. Following (Xiong et al. 2021) we use a 2-layer transformer model with 64 embedding dimensions, 128 hidden dimensions, and 2 attention heads for all experiments. Mean pooling is used in all classifiers.

For comparable computation complexity, we control the number of features used in all methods, which leads to 256 as the number of features in Skeinformer, 256 as k in Linformer, 256 as the number of landmarks in Nyströmformer, $(256/\log n)$ as the factor in Informer, and 256 as the number of features in Performer. Additionally, the number of random blocks and block size in Big Bird are by default 3 and 64, under which setting Big Bird will visit $640 \cdot n$ elements in the attention matrix while other models visit $256 \cdot n$ elements. A clearer complexity evaluation on the FLOPs of each method is provided in Appendix A.2.

We use Adam optimizer (Kingma and Ba 2015) with a learning rate of $1e - 4$. Batch size is selected conditioned on the memory requirements of Skeinformer, which leads to 128 for Text Classification, 256 for ListOps, 64 for Document Retrieval, 512 for Pathfinder and 256 for Image. For methods reporting out-of-memory errors, we apply gradient accumulation and report the accumulated steps in Appendix. Instead of setting a fixed epoch number, we train all models until convergence with a stopping strategy (if better perfor-

Models	Text			ListOps			Retrieval			Pathfinder			Image		
	step	time	accu	step	time	accu	step	time	accu	step	time	accu	step	time	accu
Standard	11	51	8	9	22	4	20	53	4	21	14	4	4	21	4
· w/o dropout	6	39	16	6	20	8	16	42	8	18	12	8	4	15	8
V-mean	8	4	1	10	4	1	27	4	1	16	4	1	7	4	1
BigBird	6	21	2	9	17	2	15	22	2	17	18	2	3	19	1
Performer	30	3	2	10	9	2	13	12	2	9	10	2	5	9	1
Nystromformer	12	12	2	10	12	2	17	13	2	23	20	4	3	10	1
Reformer	7	11	2	14	8	2	26	11	1	24	9	2	5	12	1
Linformer	7	8	2	11	6	2	23	8	1	7	7	2	4	7	1
· w/ unreduced JLT	6	37	16	4	21	8	24	36	16	12	15	4	4	22	2
Informer	8	33	8	10	22	8	25	37	4	9	26	8	7	25	2
· w/ mask	7	26	4	4	22	4	31	36	2	7	16	4	5	23	2
Skeinformer	6	10	2	7	10	2	20	11	1	18	9	2	6	12	1
· w/ US	8	8	1	3	7	1	26	7	1	19	7	1	8	8	1
· w/o RN	6	25	8	6	16	4	14	56	16	13	11	2	5	16	2
· w/ SRN	7	7	1	6	8	1	19	8	1	14	7	1	6	11	1
· w/o PSR	7	7	1	6	7	1	22	9	1	17	7	1	6	10	1

Table 2: Training steps (k), training time (minute) per thousand steps, and batch accumulation steps on LRA benchmark. Smaller training steps implies faster convergence. Less training time per thousand steps indicates higher time efficiency. Less batch accumulation steps means larger actual batch size and higher space efficiency. **US**: Uniform Sampling, **RN**: Row Normalization, **SRN**: Simple Row Normalization, **PSR**: Pilot Sampling Reutilization.

mance is not observed for 10 checking steps on the validation set we will stop the training process) and report the required steps and average time also in Appendix.

We conduct all experiments on one Tesla V100 SXM2 16GB. For numerical consistency, all experiment results are averaged across three random runs.

6.3 Results

A transformer is considered efficient when it (1) reduces space complexity and supports larger sequence length and larger batch size, (2) reduces time complexity with less training time per step and less total time to converge, and (3) shows comparable performance with vanilla softmax without much loss from approximation. Accordingly, we conclude the results shown in Table 1 and Table 2 with the following observations:

Space Efficiency: Skeinformer requires less space and enables larger batch size. Within a certain range, a larger batch size usually means more accurate gradient estimations. Therefore, we simulate the case of real-world applications of efficient transformers that models are trained with their maximum batch size conditioned on memory. In general, Skeinformer requires the least space during the training process and supports a larger batch size.

Time Efficiency: Skeinformer has consistently less time consumption. We compare the steps and total training time required for convergence. Our method takes consistently much less total training time to converge comparing to the vanilla self-attention. For example, Skeinformer brings 4.78% accuracy improvement and nearly $9\times$ speed-up on text classification over the standard method.

Fast Convergence: Skeinformer efficiently converges to the long-time limit. Regarding the training efficiency, we focus on how soon the model can attain the stationary distribution of its long-time limit (He, Liu, and Tao 2019).

The loss decay plot on ListOps in Figure 2 in Appendix A shows significant differences in the convergence rate of each method in addition to classification accuracy.

Comparable General Performance: Most $\tilde{\mathcal{O}}(n)$ attention acceleration methods have comparable or better performance with vanilla attention. After all models converge to their long-time limits, Linformer tends to have worse performance possibly due to the violation of the sketching form, while Skeinformer has the best overall performance.

The pitch of most efficient transformers above is to mimic the original transformer with a reduced computation cost. While surprising, those approximation methods tend to outperform the original transformer in most tasks. We speculate the reason behind this phenomenon is that a good approximation can recover the main signals in the original self-attention matrix, and also restrain the noise via the sparse / low-rank structure. A similar phenomenon can be found in CNN (Sanyal et al. 2018), that a low-rank regularizer, such as SVD, applied to the representation of the intermediate layers can allow the model to have lower prediction errors.

7 Conclusion

We conclude in this paper that sketching can be applied as a theoretical framework for analyzing fast attention models, through which we are able to recognize the potential improvements upon previous work. Theoretical results are provided to guarantee the high accuracy of the approximation to the original self-attention by our proposed Skeinformer. We also empirically validate the contributions of the components in Skeinformer, including column sampling, adaptive row normalization and pilot sampling reutilization, with extensive comparisons with various baseline methods and ablation methods.

8 Acknowledgments

This research is based upon work in part supported by the Office of the Director of National Intelligence (ODNI), Intelligence Advanced Research Projects Activity (IARPA), via contract No. FA8650-17-C-9116, and U.S. DARPA KAIROS Program No. FA8750-19-2-1004. This work is also in part supported by NSF grant DMS-1810831. The views and conclusions contained herein are those of the authors and should not be interpreted as necessarily representing the official policies, either expressed or implied, of DARPA, ODNI, IARPA, or the U.S. Government. The U.S. Government is authorized to reproduce and distribute reprints for governmental purposes notwithstanding any copyright annotation therein.

References

- Ailon, N.; and Chazelle, B. 2006. Approximate nearest neighbors and the fast Johnson-Lindenstrauss transform. In *Proceedings of the thirty-eighth annual ACM symposium on Theory of computing*, 557–563.
- Bao, G.; Zhang, Y.; Teng, Z.; Chen, B.; and Luo, W. 2021. G-Transformer for Document-Level Machine Translation. In Zong, C.; Xia, F.; Li, W.; and Navigli, R., eds., *Proceedings of the 59th Annual Meeting of the Association for Computational Linguistics and the 11th International Joint Conference on Natural Language Processing, ACL/IJCNLP 2021, (Volume 1: Long Papers), Virtual Event, August 1-6, 2021*, 3442–3455. Association for Computational Linguistics.
- Beltagy, I.; Peters, M. E.; and Cohan, A. 2020. Longformer: The Long-Document Transformer. *CoRR*, abs/2004.05150.
- Boucheron, S.; Lugosi, G.; and Massart, P. 2013. *Concentration inequalities: A nonasymptotic theory of independence*. Oxford university press.
- Chen, Y.; and Yang, Y. 2021. Accumulations of Projections—A Unified Framework for Random Sketches in Kernel Ridge Regression. *arXiv preprint arXiv:2103.04031*.
- Child, R.; Gray, S.; Radford, A.; and Sutskever, I. 2019. Generating Long Sequences with Sparse Transformers. *CoRR*, abs/1904.10509.
- Choromanski, K.; Likhoshesterov, V.; Dohan, D.; Song, X.; Gane, A.; Sarlós, T.; Hawkins, P.; Davis, J.; Mohiuddin, A.; Kaiser, L.; Belanger, D.; Colwell, L.; and Weller, A. 2020. Rethinking Attention with Performers. *CoRR*, abs/2009.14794.
- Cohen, M. B.; Nelson, J.; and Woodruff, D. P. 2016. Optimal Approximate Matrix Product in Terms of Stable Rank. In Chatzigiannakis, I.; Mitzenmacher, M.; Rabani, Y.; and Sangiorgi, D., eds., *43rd International Colloquium on Automata, Languages, and Programming, ICALP 2016, July 11-15, 2016, Rome, Italy*, volume 55 of *LIPIcs*, 11:1–11:14. Schloss Dagstuhl - Leibniz-Zentrum für Informatik.
- Dong, Y.; Cordonnier, J.-B.; and Loukas, A. 2021. Attention is not all you need: Pure attention loses rank doubly exponentially with depth. *arXiv preprint arXiv:2103.03404*.
- Drineas, P.; Kannan, R.; and Mahoney, M. W. 2006. Fast Monte Carlo algorithms for matrices I: Approximating matrix multiplication. *SIAM Journal on Computing*, 36(1): 132–157.
- Drineas, P.; Mahoney, M. W.; and Cristianini, N. 2005. On the Nyström Method for Approximating a Gram Matrix for Improved Kernel-Based Learning. *journal of machine learning research*, 6(12).
- Du, X.; and Cardie, C. 2020. Document-Level Event Role Filler Extraction using Multi-Granularity Contextualized Encoding. In Jurafsky, D.; Chai, J.; Schluter, N.; and Tetreault, J. R., eds., *Proceedings of the 58th Annual Meeting of the Association for Computational Linguistics, ACL 2020, Online, July 5-10, 2020*, 8010–8020. Association for Computational Linguistics.
- Ebner, S.; Xia, P.; Culkin, R.; Rawlins, K.; and Durme, B. V. 2020. Multi-Sentence Argument Linking. In Jurafsky, D.; Chai, J.; Schluter, N.; and Tetreault, J. R., eds., *Proceedings of the 58th Annual Meeting of the Association for Computational Linguistics, ACL 2020, Online, July 5-10, 2020*, 8057–8077. Association for Computational Linguistics.
- Halko, N.; Martinsson, P.; and Tropp, J. A. 2011. Finding Structure with Randomness: Probabilistic Algorithms for Constructing Approximate Matrix Decompositions. *SIAM Rev.*, 53(2): 217–288.
- Har-Peled, S.; Indyk, P.; and Motwani, R. 2012. Approximate nearest neighbor: Towards removing the curse of dimensionality. *Theory of computing*, 8(1): 321–350.
- He, F.; Liu, T.; and Tao, D. 2019. Control Batch Size and Learning Rate to Generalize Well: Theoretical and Empirical Evidence. In Wallach, H. M.; Larochelle, H.; Beygelzimer, A.; d’Alché-Buc, F.; Fox, E. B.; and Garnett, R., eds., *Advances in Neural Information Processing Systems 32: Annual Conference on Neural Information Processing Systems 2019, NeurIPS 2019, December 8-14, 2019, Vancouver, BC, Canada*, 1141–1150.
- Huang, L.; Cao, S.; Parulian, N.; Ji, H.; and Wang, L. 2021. Efficient Attentions for Long Document Summarization. In *Proceedings of the 2021 Conference of the North American Chapter of the Association for Computational Linguistics*. Association for Computational Linguistics.
- Johnson, W. B.; and Lindenstrauss, J. 1984. Extensions of Lipschitz mappings into a Hilbert space. *Contemporary mathematics*, 26(189-206): 1.
- Katharopoulos, A.; Vyas, A.; Pappas, N.; and Fleuret, F. 2020. Transformers are RNNs: Fast Autoregressive Transformers with Linear Attention. In *Proceedings of the 37th International Conference on Machine Learning, ICML 2020, 13-18 July 2020, Virtual Event*, volume 119 of *Proceedings of Machine Learning Research*, 5156–5165. PMLR.
- Kingma, D. P.; and Ba, J. 2015. Adam: A Method for Stochastic Optimization. In Bengio, Y.; and LeCun, Y., eds., *3rd International Conference on Learning Representations, ICLR 2015, San Diego, CA, USA, May 7-9, 2015, Conference Track Proceedings*.
- Kitaev, N.; Kaiser, L.; and Levskaya, A. 2019. Reformer: The Efficient Transformer. In *International Conference on Learning Representations*.
- Kitaev, N.; Kaiser, L.; and Levskaya, A. 2020. Reformer: The Efficient Transformer. In *8th International Conference on Learning Representations, ICLR 2020, Addis Ababa, Ethiopia, April 26-30, 2020*. OpenReview.net.
- Krizhevsky, A.; Hinton, G.; et al. 2009. Learning multiple layers of features from tiny images.
- Li, P.; Hastie, T. J.; and Church, K. W. 2006. Very sparse random projections. In *Proceedings of the 12th ACM SIGKDD international conference on Knowledge discovery and data mining*, 287–296.
- Li, S.; Ji, H.; and Han, J. 2021. Document-Level Event Argument Extraction by Conditional Generation. *CoRR*, abs/2104.05919.

- Linsley, D.; Kim, J.; Veerabadrán, V.; Windolf, C.; and Serre, T. 2018. Learning long-range spatial dependencies with horizontal gated recurrent units. In Bengio, S.; Wallach, H. M.; Larochelle, H.; Grauman, K.; Cesa-Bianchi, N.; and Garnett, R., eds., *Advances in Neural Information Processing Systems 31: Annual Conference on Neural Information Processing Systems 2018, NeurIPS 2018, December 3-8, 2018, Montréal, Canada*, 152–164.
- Lu, Y.; Dhillon, P. S.; Foster, D.; and Ungar, L. 2013. Faster ridge regression via the Subsampled Randomized Hadamard Transform. In *Proceedings of the 26th International Conference on Neural Information Processing Systems-Volume 1*, 369–377.
- Maas, A. L.; Daly, R. E.; Pham, P. T.; Huang, D.; Ng, A. Y.; and Potts, C. 2011. Learning Word Vectors for Sentiment Analysis. In Lin, D.; Matsumoto, Y.; and Mihalcea, R., eds., *The 49th Annual Meeting of the Association for Computational Linguistics: Human Language Technologies, Proceedings of the Conference, 19-24 June, 2011, Portland, Oregon, USA*, 142–150. The Association for Computer Linguistics.
- Merity, S.; Xiong, C.; Bradbury, J.; and Socher, R. 2017. Pointer Sentinel Mixture Models. In *5th International Conference on Learning Representations, ICLR 2017, Toulon, France, April 24-26, 2017, Conference Track Proceedings*. OpenReview.net.
- Nangia, N.; and Bowman, S. R. 2018. ListOps: A Diagnostic Dataset for Latent Tree Learning. In Cordeiro, S. R.; Oraby, S.; Pavalanathan, U.; and Rim, K., eds., *Proceedings of the 2018 Conference of the North American Chapter of the Association for Computational Linguistics, NAACL-HLT 2018, New Orleans, Louisiana, USA, June 2-4, 2018, Student Research Workshop*, 92–99. Association for Computational Linguistics.
- Qiu, J.; Ma, H.; Levy, O.; Yih, W.; Wang, S.; and Tang, J. 2020. Blockwise Self-Attention for Long Document Understanding. In Cohn, T.; He, Y.; and Liu, Y., eds., *Proceedings of the 2020 Conference on Empirical Methods in Natural Language Processing: Findings, EMNLP 2020, Online Event, 16-20 November 2020*, 2555–2565. Association for Computational Linguistics.
- Radev, D. R.; Muthukrishnan, P.; Qazvinian, V.; and Abu-Jbara, A. 2013. The ACL anthology network corpus. *Lang. Resour. Evaluation*, 47: 919–944.
- Rahimi, A.; Recht, B.; et al. 2007. Random Features for Large-Scale Kernel Machines. In *NIPS*, volume 3, 5. Cite-seer.
- Roy, A.; Saffar, M.; Vaswani, A.; and Grangier, D. 2021. Efficient Content-Based Sparse Attention with Routing Transformers. *Trans. Assoc. Comput. Linguistics*, 9: 53–68.
- Sanyal, A.; Kanade, V.; Torr, P. H.; and Dokania, P. K. 2018. Robustness via deep low-rank representations. *arXiv preprint arXiv:1804.07090*.
- Tay, Y.; Dehghani, M.; Abnar, S.; Shen, Y.; Bahri, D.; Pham, P.; Rao, J.; Yang, L.; Ruder, S.; and Metzler, D. 2020a. Long Range Arena: A Benchmark for Efficient Transformers. *CoRR*, abs/2011.04006.
- Tay, Y.; Dehghani, M.; Bahri, D.; and Metzler, D. 2020b. Efficient Transformers: A Survey. *CoRR*, abs/2009.06732.
- Vaswani, A.; Shazeer, N.; Parmar, N.; Uszkoreit, J.; Jones, L.; Gomez, A. N.; Kaiser, L.; and Polosukhin, I. 2017. Attention is All you Need. In Guyon, I.; von Luxburg, U.; Bengio, S.; Wallach, H. M.; Fergus, R.; Vishwanathan, S. V. N.; and Garnett, R., eds., *Advances in Neural Information Processing Systems 30: Annual Conference on Neural Information Processing Systems 2017, December 4-9, 2017, Long Beach, CA, USA*, 5998–6008.
- Vershynin, R. 2010. Introduction to the non-asymptotic analysis of random matrices. *arXiv preprint arXiv:1011.3027*.
- Wainwright, M. J. 2019. *High-dimensional statistics: A non-asymptotic viewpoint*, volume 48. Cambridge University Press.
- Wang, S.; Li, B. Z.; Khabsa, M.; Fang, H.; and Ma, H. 2020a. Linformer: Self-Attention with Linear Complexity. *CoRR*, abs/2006.04768.
- Wang, S.; Zhou, L.; Gan, Z.; Chen, Y.; Fang, Y.; Sun, S.; Cheng, Y.; and Liu, J. 2020b. ClusterFormer: Clustering-based Sparse Transformer for Long-Range Dependency Encoding. *CoRR*, abs/2009.06097.
- Williams, C.; and Seeger, M. 2001. Using the Nyström method to speed up kernel machines. In *Proceedings of the 14th annual conference on neural information processing systems*, CONF, 682–688.
- Wolf, T.; Debut, L.; Sanh, V.; Chaumond, J.; Delangue, C.; Moi, A.; Cistac, P.; Rault, T.; Louf, R.; Funtowicz, M.; and Brew, J. 2019. HuggingFace’s Transformers: State-of-the-art Natural Language Processing. *CoRR*, abs/1910.03771.
- Woodruff, D. P.; et al. 2014. Sketching as a Tool for Numerical Linear Algebra. *Foundations and Trends® in Theoretical Computer Science*, 10(1–2): 1–157.
- Xiao, W.; and Carenini, G. 2019. Extractive Summarization of Long Documents by Combining Global and Local Context. In Inui, K.; Jiang, J.; Ng, V.; and Wan, X., eds., *Proceedings of the 2019 Conference on Empirical Methods in Natural Language Processing and the 9th International Joint Conference on Natural Language Processing, EMNLP-IJCNLP 2019, Hong Kong, China, November 3-7, 2019*, 3009–3019. Association for Computational Linguistics.
- Xiong, Y.; Zeng, Z.; Chakraborty, R.; Tan, M.; Fung, G.; Li, Y.; and Singh, V. 2021. Nyströmformer: A Nyström-Based Algorithm for Approximating Self-Attention. *CoRR*, abs/2102.03902.
- Yang, Y.; Pilanci, M.; Wainwright, M. J.; et al. 2017. Randomized sketches for kernels: Fast and optimal nonparametric regression. *The Annals of Statistics*, 45(3): 991–1023.
- Zaheer, M.; Guruganesh, G.; Dubey, K. A.; Ainslie, J.; Alberti, C.; Ontañón, S.; Pham, P.; Ravula, A.; Wang, Q.; Yang, L.; and Ahmed, A. 2020. Big Bird: Transformers for Longer Sequences. In Larochelle, H.; Ranzato, M.; Hadsell, R.; Balcan, M.; and Lin, H., eds., *Advances in Neural Information*

Processing Systems 33: Annual Conference on Neural Information Processing Systems 2020, NeurIPS 2020, December 6-12, 2020, virtual.

Zhou, H.; Zhang, S.; Peng, J.; Zhang, S.; Li, J.; Xiong, H.; and Zhang, W. 2020. Informer: Beyond Efficient Transformer for Long Sequence Time-Series Forecasting. *CoRR*, abs/2012.07436.

A Further experiment results

A.1 Details of training time

Table 3 reports the total training time for one random run on each task. Our method takes consistently much less total training time to converge compared to the vanilla self-attention.

In the experiments, the batch size is selected conditioned on the memory requirements, which leads to 128 for Text Classification, 256 for ListOps, 64 for Document Retrieval, 512 for Pathfinder, and 256 for Image. For methods reporting out-of-memory errors, we apply gradient accumulation of appropriate steps. We show the actual batch size during gradient accumulation steps in the training process in Table 4. SKEINFORMER requires less space for training and thus supports the larger batch size comparing to the vanilla self-attention.

A.2 FLOPs

We conclude in this subsection the floating point operations (FLOPs) of each candidate model (excluding Reformer and the ablation models) in Section 6 in the main paper. To ease the notation, given the sequence length n , we fix $p = 32, d = 256$. Assuming the matrices $\mathbf{Q}, \mathbf{K}, \mathbf{V}$ are given and omitting the non-leading term, we report the FLOPs of each model in Table 5. We additionally comment that Reformer is excluded from the table because its FLOPs are not fixed and depend on the frequency of collision after hashing of tokens, which changes with the input sequence. Table 2 in the main paper empirically shows its average runtime per one thousand steps (and thus FLOPs) are close to the other models.

A.3 Validation loss

We present the loss decay plots on all tasks in Figure 2. In the first subplot for the text classification task, we note all the methods quickly overfit the dataset. In all the other plots, our methods show the ability to both efficiently converge to the long-time limit and find better local minima with lower validation loss.

B Proof of Lemma 1

Proof. For each column $\mathbf{B}^{(i)}$, we first define a discrete random variable X_i , that with probability $\frac{1}{n}$, $X_i = b_{ji}, \forall j \in [n]$, where b_{ji} is the j -th element in $\mathbf{B}^{(i)}$. Since all the elements in \mathbf{B} are bounded (within the range $[0, 1]$) due to the row normalization in softmax, we infer that for any $i \in [n], X_i^2 \in [0, 1]$ is a sub-Gaussian random variable with parameter $\sigma = \frac{1}{2}$ (Wainwright 2019). Combine the conclusion with the assumption that $\mathbb{E} X_i^2 \leq C$, we have

$$\frac{X_i^2}{\mathbb{E} X_i^2} \sim \text{sub-Gaussian} \left(\sigma^2 = \frac{1}{4C^2} \right). \quad (7)$$

Then we uniformly sample d indexes $\{j_k\}_{k=1}^d$'s with replacement, and we estimate the squared norm of each column with the unbiased estimator $Y_i = \frac{n}{d} \sum_{k=1}^d b_{j_k i}^2$. We remark Y_i has the same distribution as $\frac{n}{d} \sum_{k=1}^d X_{i,(k)}^2$, where

$X_{i,(k)}$'s are d i.i.d. copies of X_i . Therefore through a linear transform of Equation (7) we can derive that

$$\frac{Y_i}{n \mathbb{E} X_i^2} \sim \text{sub-Gaussian} \left(\sigma^2 = \frac{1}{4C^2 d} \right). \quad (8)$$

Notice different Y_i 's may not be independent since they all rely on the same d rows in \mathbf{B} . However, we can still apply the maximal sub-Gaussian inequality (Boucheron, Lugosi, and Massart 2013) to have:

$$\mathbb{P} \left\{ \max_{i \in [n]} \left| \frac{Y_i}{n \mathbb{E} X_i^2} - 1 \right| > \frac{1}{2} \right\} \leq 2ne^{-\frac{C^2 d}{2}}. \quad (9)$$

If the high probability bound holds that $\max_{i \in [n]} \left| \frac{Y_i}{n \mathbb{E} X_i^2} - 1 \right| \leq \frac{1}{2}$, we directly have that our estimators $Y_i \in [\frac{1}{2} \|\mathbf{B}^{(i)}\|^2, \frac{3}{2} \|\mathbf{B}^{(i)}\|^2], \forall i \in [n]$. In that case, the estimated sub-sampling probabilities satisfy that

$$\begin{aligned} \hat{p}_i &= \frac{Y_i^{\frac{1}{2}} \|\mathbf{V}^{(i)}\|}{\sum_{i'=1}^n Y_{i'}^{\frac{1}{2}} \|\mathbf{V}^{(i')}\|} \geq \frac{\sqrt{1/2} \|\mathbf{B}^{(i)}\| \|\mathbf{V}^{(i)}\|}{\sqrt{3/2} \|\mathbf{B}^{(i)}\| \|\mathbf{V}^{(i')}\|} \\ &= \sqrt{\frac{1}{3}} p_i, \forall i \in [n], \end{aligned}$$

where p_i 's are the optimal probabilities defined in Equation (3) in the main paper.

In that case, to prove the lemma it suffices to pick a big enough sub-sample size d such that the right-hand side of Inequality (9) is smaller than δ . Simply solving the inequality leads to the desired result $d \geq \frac{2}{C^2} \log(\frac{2n}{\delta})$. \diamond

Models	Text		ListOps		Retrieval (64)		Pathfinder		Image	
	steps	time	steps	time	steps	time	steps	time	steps	time
Standard	10.67	540.00	8.53	190.29	19.80	1,054.67	21.40	297.78	4.33	92.73
· w/o dropout	5.67	223.79	5.58	108.90	16.30	682.72	17.58	207.14	4.23	63.01
V-mean	8.00	28.92	9.77	40.46	26.50	103.41	15.60	57.27	7.38	32.77
BigBird	6.00	123.52	9.07	156.68	14.90	323.83	17.47	311.40	3.20	60.28
Performer	30.33	79.64	9.90	92.14	12.50	156.22	8.83	91.91	5.13	45.87
Nystromformer	11.50	140.02	9.87	121.19	17.10	228.26	22.60	442.59	2.92	30.06
Reformer	6.67	70.17	14.20	117.55	26.40	297.59	24.13	223.28	4.78	56.84
Linformer	6.50	51.38	11.43	71.48	23.20	187.51	7.30	50.35	4.25	28.27
· w/ unreduced JLT	6.25	230.46	3.98	85.43	23.85	856.83	12.01	182.18	4.30	94.75
Informer	8.00	265.06	10.13	221.79	24.70	901.99	9.47	247.50	6.72	167.37
· w/ padding mask	7.00	181.61	4.20	90.31	30.90	1,110.98	7.02	110.83	5.10	115.14
Skeinformer	6.17	59.23	7.32	70.71	20.40	216.36	17.89	165.54	5.57	66.02
· w/ uniform sampling	8.00	60.79	3.20	21.30	26.10	174.96	18.72	136.05	7.67	59.52
· w/o row normalization	6.17	154.31	5.90	94.54	13.80	768.97	13.21	146.88	4.50	69.83
· w/ simple row normalization	6.67	45.32	6.27	51.12	19.30	155.07	13.62	93.19	5.78	65.17
· w/o pilot sampling reutilization	6.50	46.47	6.25	45.68	22.20	192.69	16.64	117.99	6.23	63.51

Table 3: Training steps (k) and total training time (minute) on LRA benchmark.

Models	Text (128)		ListOps (256)		Retrieval (64)		Pathfinder (512)		Image(256)	
	bz	accu	bz	accu	bz	accu	bz	accu	bz	accu
Standard	16	8	64	4	16	4	128	4	64	4
· w/o dropout	8	16	32	8	8	8	64	8	32	8
V-mean	128	1	256	1	64	1	512	1	256	1
BigBird	64	2	128	2	32	2	256	2	256	1
Performer	64	2	128	2	32	2	256	2	256	1
Nystromformer	64	2	128	2	32	2	128	4	256	1
Reformer	64	2	128	2	64	1	256	2	256	1
Linformer	64	2	128	2	64	1	256	2	256	1
· w/ unreduced JLT	8	16	32	8	4	16	128	4	128	2
Informer	16	8	32	8	16	4	64	8	128	2
· w/ padding mask	32	4	64	4	32	2	128	4	128	2
Skeinformer	64	2	128	2	64	1	256	2	256	1
· w/ uniform sampling	128	1	256	1	64	1	512	1	256	1
· w/o row normalization	16	8	64	4	4	16	256	2	128	2
· w/ simple row normalization	128	1	256	1	64	1	512	1	256	1
· w/o pilot sampling reutilization	128	1	256	1	64	1	512	1	256	1

Table 4: Actual batch size (bz) during gradient accumulation steps (accu) under constraints of memory usage.

Table 5: The leading terms of FLOPs in computing attention

Models	FLOPs
Standard	$2n^2p$
Big Bird	$5ndp$
Performer	$3ndp$
Nystromformer	$4ndp$
Linformer	$4ndp$
Informer	$3ndp$
Skeinformer	$4ndp$

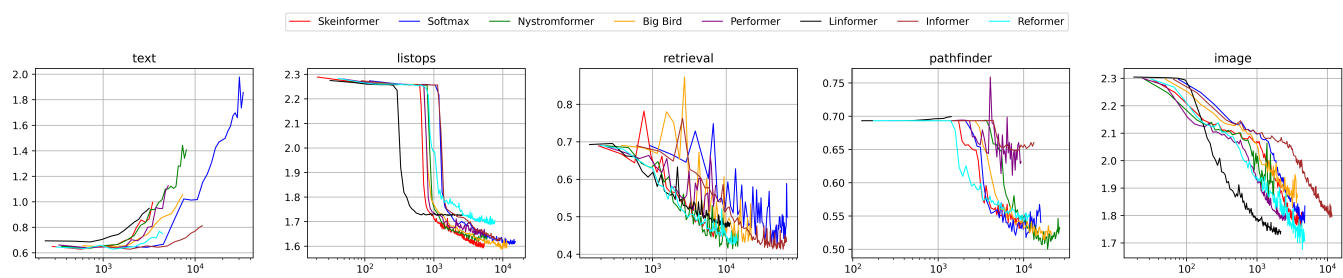


Figure 2: Validation loss changes with regard to training time.